Simplified Finite Element Simulation of a SAW Hydrogen Sensor using COMSOL Multiphysics

N. Rama Krishnan[1], Harshal B Nemade[*, 1, 2] and Roy Paily[3]
[1]Centre for Nanotechnology, Indian Institute of Technology Guwahati, India, [2] Department of Electronics and Communication Engineering, Indian Institute of Technology, India
*Corresponding author: harshal@iitg.ernet.in

Abstract: In this paper, we discuss a simplified finite element method (FEM) simulation of surface acoustic wave (SAW) delay line hydrogen sensor using COMSOL Multiphysics. A delay line SAW sensor consists of a transmitting interdigital transducer (IDT) and a receiving IDT separated by a few wavelengths. In this paper, the number of degrees of freedom (DOF) to solve for the SAW delay line sensor model is minimized by providing periodic boundary conditions to the transmitting IDT, which is a one finger structure. Further a palladium thin film is coated over the delay line. The palladium film transforms to palladium hydride in the presence of hydrogen. This change in palladium properties are provided to the assumed thin film over the delay line. The time domain analysis of SAW sensor with and without the presence of hydrogen is performed and change in velocity of the SAW is observed.

Keywords: MEMS, SAW Sensor, Hydrogen sensor, IDT.

1. Introduction

Surface acoustic waves (SAWs) are ultrasonic waves propagating along the surface of solids. An interdigital transducer (IDT) performs the function of conversion of electrical energy to mechanical energy and vice versa. IDT is a comb-shaped metallic structure fabricated over the piezoelectric substrate. A voltage applied to the IDT produces dynamic strains in the substrate and initiates elastic waves that travel along the surface. Various types of SAW devices based on rayleigh wave, SH-SAW, love wave, acoustic plate mode (APM), flexural plate wave (FPM) have been explored for sensors, actuators and telecommunication applications [1] [2].

A delay line SAW device for sensor applications consists of a transmitting IDT and a receiving IDT separated by a few wavelengths. Standing waves produced by the transmitter IDT give rise to propagation of SAW in the both directions of the IDT [2]. Various SAW sensors are reported based on the principle of change in velocity and amplitude of the SAW for change in physical properties of the sensing medium such as mass loading, conductivity, permittivity, viscosity and strain. Simulations of such devices help in visualizing the SAW sensor response and optimizing the SAW device structure. Simulation of SAW devices can be performed various methods such as finite element method (FEM), equivalent circuit method and coupling of mode method. FEM simulation of SAW sensors gives insight physics of these devices. Few literatures have discussed about FEM simulation of SAW sensors such as 3D FEM analysis of SAW hydrogen sensor using ANSYS by Atashbar *et al* [3]. FEM Simulation of SAW propagation over layered substrates has been shown by Ippolito *et al* [4]. Effect of film properties over mass sensitivity of a SAW sensor was studied using FEM simulation by Wang *et al* [5]. In this paper we discuss the simulation of SAW delay line hydrogen sensor using FEM based COMSOL Multiphysics software, where the sensitivity of mass loading is studied. In concern with memory usage of the machine and computation time, we have assumed one finger model transmitting IDT. As the fingers of IDT are periodic in nature, periodic boundary conditions are applied for the boundaries of the transmitting IDT. Receiver IDT consists of one electrode to detect the SAW passing by. The shift in frequency of the delay line oscillator can be related to the density and elastic modulus by equation 3 [6].

$$\Delta f = (k_1 + k_2) f_0^2 h \rho_f - k_2 f_0^2 h \left\{ \frac{4\mu'(\lambda' + \mu')}{v^2(\lambda' + 2\mu')} \right\} \quad (1)$$

where, Δf is the shift in frequency, k_1 and k_2 are piezoelectric crystal constants, ρ_f is the film density, h is the height of the film, λ' and μ' are bulk modulus and shear modulus. It can be seen that first term in right hand side of equation 3 depends on density of the film and second term depends on the elastic property of the film. In

this simulation a palladium film is coated over the delay line. The simulation of SAW sensor is performed by varying the density, youngs modulus and volume of the film assumed over the delay line. Piezoelectric crystal constitutive relations are shown in section 2, material and structure considered for the simulation is briefed in section 3, simulation procedure, results and conclusion are discussed in sections 4, 5, and 6 respectively.

2. Piezoelectric model

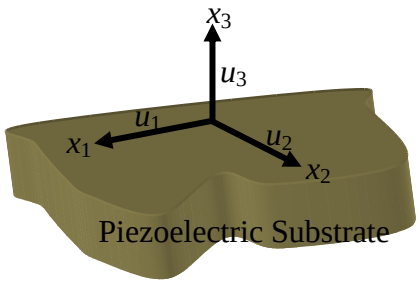

Figure 1. Coordinate system for the wave solutions.

FEM model of piezoelectric material explained in the literatures [7] [8]**.** The relation between the stress, strain, electric field, and electric displacement field in a stress-charge of a piezoelectric crystal is given by the piezoelectric constructive equations equation (1 and 2)

$$T_{ij} = C^{E}_{ijkl} \,.\, S_{kl} - e_{kij} \,.\, E_k \qquad (2)$$

$$D_i = e_{ikl} \,.\, S_{kl} - \varepsilon^{s}_{ik} \,.\, E_k \qquad (3)$$

Where, T_{ij} Represents the stress vector, C^{E}_{ijkl} is the elasticity matrix, e_{kij} is the strain vector, ε^{s}_{ik} is the permittivity matrix, E_k the electric field vector, S_{kl} is the strain vector, D_i is the electrical displacement. The degrees of freedom (dependent variables) are the global displacements u_1, u_2, and u_3 in the global x_1, x_2, and x_3 directions(figure 1), and the electric potential V, can be obtained by solving the Newton's and Maxwell equation related to equations (1 and 2)are given below,

$$\sum_{jkl} C^{E}_{ijkl} \frac{\partial^2 u_l}{\partial x_j \partial x_k} + \sum_{jk} e_{kij} \frac{\partial^2 V}{\partial x_j \partial x_k} = \rho \frac{\partial^2 u_i}{\partial t^2} \qquad (4)$$

$$\sum_{kl} e_{jkl} \frac{\partial^2 u_l}{\partial x_j \partial x_k} + \sum_{jk} \varepsilon^{s}_{jk} \frac{\partial^2 V}{\partial x_j \partial x_k} = 0 \qquad (5)$$

for i, j, k, l = 1,2 and 3.

The Rayleigh elastic wave displacement has components in surface-normal and surface-parallel directions with respect to the direction of the wave propagation. The particle in the upper surface takes elliptical path having both the components.

3. Simulation methodology

We have considered the total SAW hydrogen sensor as a 2D plain strain structure as shown in the Figure 2. The intensity of the SAW is confined more at the surface of substrate and displacement along x_2 direction is zero for rayleigh SAW [1]. The SAW model considered in this simulation consists of 3 geometries, the transmitter IDT ($G1$) to generate the standing rayleigh waves, delay line with a receiving electrode as receiver IDT ($G2$). Further delay line is extended to two wavelengths and critical damping is assumed for the extended substrate ($G3$) to avoid reflections at the end of the delay line. YZ lithium niobate is assumed for the substrate and its elastic constants, permittivity constants, stress constants are taken from warner *et al* [8]. A delay line of 120.8 µm in length and 174.4 µm in height is considered. A palladium thin film of density 12000 Kg/m^3 and youngs modulus of 129 Gpa with dimensions of 52.32 µm x 1µm is placed 8.75 µm from IDT over the delay line. Massless electrodes are assumed for the transmitting and receiving finger to avoid mass loading due to these electrodes. As the fingers in IDTs are periodic, appropriate periodic boundary conditions are applied for the transmitting IDT using the equation 6 [9].

$$\Gamma_L(\mathbf{u}, V) = \Gamma_R(\mathbf{u}, V)\, exp(-j2\pi\, \gamma n) \qquad (6)$$

where, Γ_L and Γ_R denotes left side and right side boundary of the transmitter as shown in the figure 2, n is a positive integer, γ is complex prorogation constant, **u** denotes the SAW displacement vector, V is the potential. 2D mapped mesh is applied for the geometries ($G1$, $G2$, and $G3$). The mesh has total 26286 degrees of freedom.

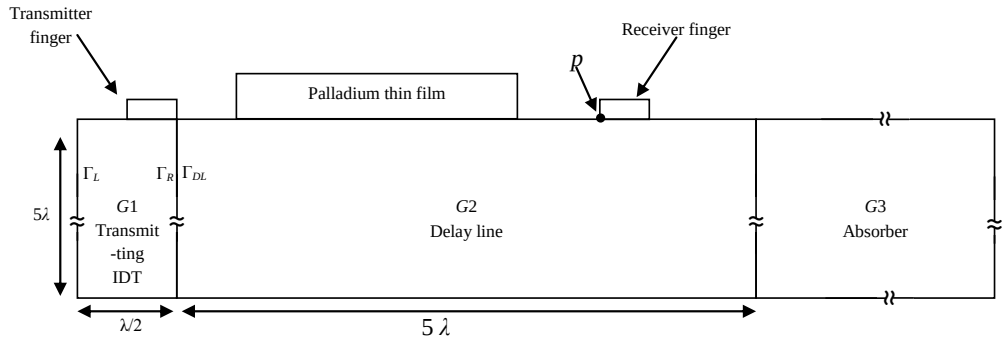

Figure 2. Section of SAW sensor geometry considered for the simulation.

Time domain analyses of SAW hydrogen sensor are performed in two stages. In the first stage the absence of SAW hydrogen sensor is simulated. In the second stage 3 % absorption of hydrogen by palladium film to palladium hydride is simulated, where the palladium thin film density is decreased by 2 %, volume is increased by 10 % and youngs modulus is reduced by 14 % [3][10] and time domain analysis of SAW delay line with modified properties of thin film is performed.

4. Results and discussions

Frequency response analysis is performed for the transmitting IDT and synchronous frequency of the transmitter found to be 98 MHz. Hence a 98 MHz, 20 V peak to peak sinusoidal signal is

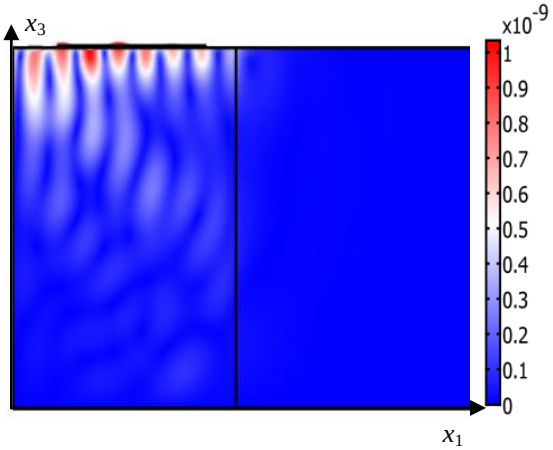

Figure 3. Total displacement profile of SAW in the delay line.

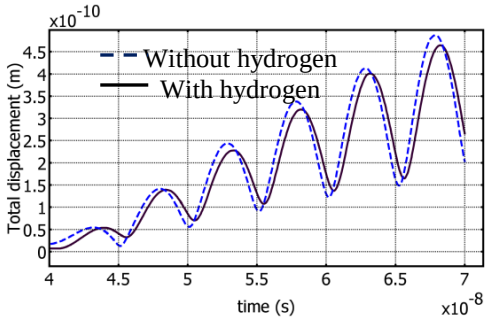

Figure 4. Total displacement of SAW recorded at the receiver point in the presence and absence of hydrogen.

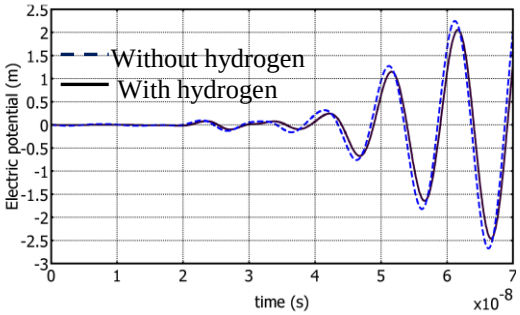

Figure 5. Electric potential of SAW recorded at the receiver point in presence and absence of hydrogen.

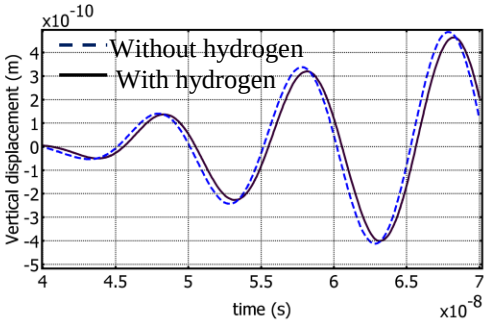

Figure 6. Vertical displacement of SAW recorded at the receiver point in presence and absence of hydrogen.

applied to the electrode of transmitting IDT and time domain analysis of *G*1 alone is performed for 70 ns. Further the simulated displacement and potential at the boundary Γ_R are stored and provided to Γ_{DL} boundary of the delay line for the further two stage of analysis of SAW hydrogen sensor. The displacement and electric potential at receiving point *p* (see figure 2) are recorded in both the stages as discussed in section 3. Total displacement of SAW is calculated by equation,

$$\text{Total displacement} = \sqrt{|u_1|^2 + |u_2|^2} \quad (7)$$

Figure 3 shows the profile of SAW total displacement over the delay line, for simplicity wave propagation over *G*2 and *G*3 alone is shown in figure 3. Figure 4 shows the total displacement recorded at the receiver electrode for the presence and absence of hydrogen. It can be seen that SAW displacements amplitude are in the order of 10^{-10}. The recorded SAW electric potential, vertical displacement for the presence and absence of hydrogen as discussed in section 3 are shown in figure 5 and 6. It is evident that there is a significant attenuation and delay of SAW due to change in properties of the palladium film. It can be seen from figure 5 that SAW has taken 35 ns to reach the receiver electrode. From figure 5 it can be observed that the vertical displacement of SAW in presence of hydrogen is delayed by 0.45 ns when compared to absence of hydrogen.

5. Conclusions

A simplified SAW delay line hydrogen sensor is modeled and simulated using FEM based software COMSOL Multiphysics. The number of degrees of freedom (DOF) to solve for the FEM model of SAW hydrogen sensor is reduced by following reasons, simulation of whole transmitter is avoided by the application of periodic boundary conditions to a single electrode structure and receiver IDT has one finger to detect the SAW passing by. A delay of 0.45 ns is observed for the 3 % absorption of hydrogen by the palladium film compared with absence of hydrogen. The model can be further extended to study the various other aspects of SAW sensor.

6. References

1. J. W. Gardner, V. K. Vardhan, O. O. Awadelkarim, *Microsensors, MEMS, and Smart Devices*, 303–416. John Wiley & Sons, England (2001)
2. D. S. Ballantine, R. M. White, S. I. Martin, A. I. Ricco, E. T. Zellers, G. C. Frye, H. Wohltjen, *Acoustic Waves Sensors Theory, Design, and Physico–Chemical Applications*. Academic Press (1997)
3. M. Z. Atashbar, B. J. Bazuin, M. Simpeh, S. Krishnamurthy, 3D FE simulation of H_2 SAW gas sensor, *Sensors and Actuators B*, **111-112**, 213–218 (2005)
4. S. J. Ippolitto, K. Kalantar-Zadeh, D. A. Powell, W. Wloderski, A 3- dimensional finite element approach for simulating acoustic wave propagation in layered SAW devices, *IEEE Ultrasonics Symposium*, 303 – 306 (2003)
5. X. Wang, G. Xu, Numerical study of the effects of film properties to the mass sensitivity of surface acoustic wave sensors, *IEEE Ultrasonics Symposium*, 442 – 448 (2005)
6. V. K. Varadan. K. J. Vinoy and S. Gopalakrishnan, *Smart Material Systems and MEMS: Design and Development Methodologies*, John Wiley & Sons, England (2006)
7. *COMSOL Multiphysics User Guide* Ver 3.4, (2005)
8. A. W. Warner, M. Onoe, and G. A. Coquin, Determination of elastic and piezoelectric constants for crystals in class (3M), *The journal of the acoustical society of America*, **42**, 1223-1231 (1968)
9. M. Hofer, N. Finger, G. Kovacs, J. Schoberl, S. Zaglmayr, U. Langer, and R. Lerch, Finite-element simulation of wave propagation in periodic piezoelectric SAW structures, *IEEE Transactions on Ultrasonics, Ferroelectrics, and Frequency Control*, **53**, 1192–1201 (2006)
10. A. Fabre, E. Finot, J. Demoment, S. Contreras, In situ measurement of elastic properties of PdHx, PdDx, and PdTx, *Journal of alloys and Compounds*, 356-357, (2003)